

Study on the Mechanical Properties of Cladding Layers Based on First-Principles and JMatPro

Xutao Zhao, Zixue Guo, Guohe Li

College of Mechanical Engineering, Tianjin University of Technology and Education,
Tianjin, China

OFFSHORE OIL ENGINEERING CO., LTD., Tianjin, China

Abstract: This study introduces a novel approach for determining the mechanical properties of Ni-based cladding layers by combining first-principles calculations with JMatPro software. This method offers a new perspective for developing constitutive models used in finite element simulations. First-principles calculations were employed to evaluate the atomic structure and fundamental mechanical properties of Ni-based alloys. The results were then integrated with JMatPro's thermodynamic calculations and material property database to predict the mechanical properties of the cladding layer. Subsequently, the Johnson-Cook constitutive parameters were fitted. This approach enhances the accuracy of the constitutive parameters while significantly reducing both experimental costs and time. The findings demonstrate that this method effectively supports the precise characterization of material properties in finite element simulations, providing a theoretical foundation for optimizing the cutting simulations of Ni-based cladding layers.

Keyword: first-principles, JMatPro, mechanical properties, Johnson-Cook constitutive

1 INTRODUCTION

Ni-based alloy powders are widely studied and used in laser cladding due to their excellent wettability, corrosion resistance, high-temperature self-lubrication, and cost-effectiveness^[1]. However, the high hardness and inhomogeneous microstructure of Ni-based cladding layers present challenges for subsequent machining processes. Traditional cutting experiments are time-consuming, labor-intensive, and costly. In contrast, the finite element method (FEM) has become a powerful tool for investigating the machining processes of cladding layers. The accuracy of FEM simulations relies heavily on a reliable material constitutive model^[2]. Consequently, further research is needed to determine the mechanical properties of laser-cladded materials, providing a solid foundation for FEM-based machining simulations. Many researchers have obtained the mechanical properties of cladding layers through experimental methods. For example, Zhou Yuecheng^[3], Yang^[4], and others used quasi-static tensile tests to obtain the stress-strain relationship and develop constitutive equations. However, the mechanical properties obtained from this method cannot accurately describe the high strain-rate flow behavior of materials during the cutting process. Xie Zhongya^[5], Wang^[6], and others used split-Hopkinson pressure bar tests to obtain stress-strain curves under different strain rates and temperatures. However, this method presents challenges in sample preparation and incurs high experimental costs. Integrating first-principles calculations with JMatPro to determine the mechanical properties of the cladding layer effectively mitigates these issues and reduces costs, making it a viable approach for developing constitutive models for laser-cladded materials.

In recent years, the application of first-principles calculation in materials science has become more and more extensive, which can reveal the electronic structure and mechanical properties of materials from the atomic scale. Meanwhile, JMatPro, a software based on thermodynamics and material databases, can predict the properties of various alloys. This study combines first-principles calculations with JMatPro software to propose a novel method for determining the mechanical properties of Ni-based cladding layers. The approach aims to provide reliable constitutive parameters for finite element simulations and offer theoretical guidance for material design and optimization.

2 INTRODUCTION OF MODELING SOFTWARE

In this study, the crystal model of Ni-based alloys was constructed using the first-principles calculation software Material Studio (MS). Developed and released by Accelrys in 2000, MS is primarily used for solving computational problems in materials science^[7]. The simulations cover a range of topics, including catalysts, polymers, solids and surfaces, interfaces, crystal structures and diffraction, as well as chemical reactions. This molecular simulation software is compatible with both Windows and Linux platforms, making it suitable for various computational environments, and it features an intuitive interface that is easy to use. The first-principles calculations in this study were carried out using the CASTEP package within MS^[8]. CASTEP is a quantum mechanical program based on density functional theory (DFT). Its main functions include predicting lattice constants, optimizing crystal structures, forecasting various physical and chemical properties, and calculating electronic structures and phonon spectra. As a result, CASTEP is widely used in the study of metals, intermetallic compounds, alloys, ceramics, and semiconductors, making it one of the most commonly used simulation tools in computational materials science today.

3 CONVERGENCE TESTING

In computational numerical simulations, convergence is one of the key indicators used to assess the feasibility of an algorithm. An algorithm that does not converge is not practical for computation. Therefore, convergence testing is an essential step before performing simulations of specific structures and properties. For first-principles calculations, convergence testing primarily includes testing the cutoff energy and the k-point convergence^[9]. The choice of cutoff energy and k-points in the Brillouin zone both influences the accuracy of the final calculation results and the efficiency of the computational process. Computational efficiency is a critical factor for all computational methods. On one hand, higher computational precision demands greater performance from the computer, while lower precision challenges the authenticity of the results. Finding reasonable computational parameters that meet both the performance requirements of the computer, and the accuracy requirements is crucial. In first-principles calculations, the size of the cutoff energy directly affects the calculation accuracy. As the cutoff energy increases, accuracy improves. Similarly, the selection of k-points is essential for integration calculations. The k-points are divided into reciprocal spaces along the a, b, and c directions. A higher value for the first k-point indicates more integration points along a direction, leading to higher computational accuracy, and similarly for the other directions. Therefore, this section first examines the convergence of both the cutoff energy and k-point selection.

(1) Cut-off Energy convergence testing

The purpose of the cut-off energy convergence test is to evaluate the convergence accuracy. As energy increases, the convergence accuracy improves. Typically, the convergence criterion is that the energy per

atom reaches 0.001 eV/atom. This study adopts this as the standard for convergence testing. For the cutoff energy convergence test, the k-point is fixed, and the cut-off energy is gradually increased until the system's energy stabilizes. In this study, a $2 \times 2 \times 2$ k-point mesh was chosen for the test. The cut-off energy started at 300 eV, with increments of 50 eV, resulting in several sets of cutoff energy test data, as shown in Table 1. The relationship between cutoff energy and steady-state energy, derived from the computational data, is depicted in Figure 1.

Table1 Cut-off Energy test data

No.	Energy Cut-off(eV)	Final Energy (eV)
1	300	-43223.75701443
2	350	-43225.96795819
3	400	-43226.04188014
4	450	-43226.13040228
5	500	-43226.19967295
6	550	-43226.21883692
7	600	-43226.23025784

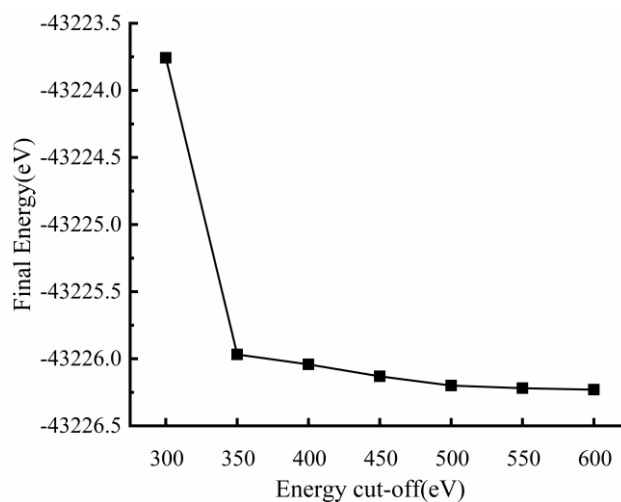


Fig.1 Relationship between Cut-off Energy and Final Energy

As clearly shown in the figure, when the cut-off energy reaches 500 eV, the energy stabilizes. Since the number of atoms in the calculated structure is 32, the difference between the current and previous results is considered negligible (less than 32 meV), indicating that the convergence condition has been met. Therefore, in this study, a cut-off energy of 500 eV was chosen for all subsequent calculations.

(2)K-point convergence testing

Before conducting a large number of first-principles calculations on the system under study, it is essential to consider the convergence of the calculation results with respect to the number of k-points. Without determining the appropriate number of k-points, reproducibility of the computational results becomes challenging. Therefore, testing the convergence with respect to k-points is critical. Based on relevant

data, the k-point convergence of the calculation model in this study was tested, and several sets of k-point test data are provided in Table 2. The curve showing the relationship between steady-state energy and the number of k-points, derived from the calculated data, is shown in Figure 2.

Table 2 k-point test data

No.	k-point	Final Energy (eV)
1	1×1×1	-43225.96366044
2	2×2×2	-43226.19967295
3	3×3×3	-43225.78749802
4	4×4×4	-43225.77771774
5	5×5×5	-43225.7815951

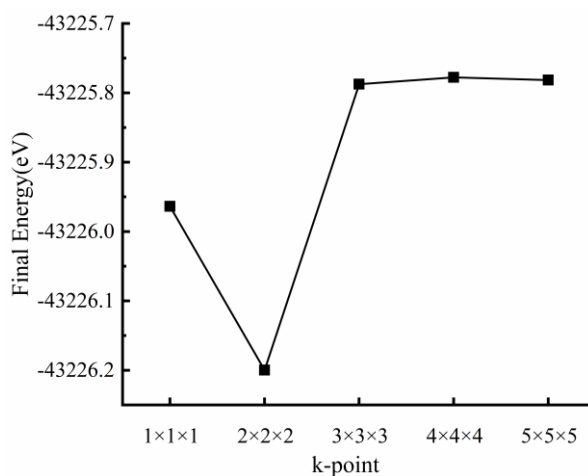


Fig.2 Relationship between k-point and Final Energy

Similarly, the convergence criterion for the k-point test is the same as that for the cutoff energy test, namely, the energy difference between two consecutive calculations must be less than 32 meV. From the curve, it is evident that the data from the third calculation meets the convergence standard. Therefore, for the computational simulations in this study, the k-point mesh selected corresponds to the third set of test data, which is 3×3×3.

4 STRUCTURAL OPTIMIZATION

A stable structure is the foundation for calculating various properties. A structure is considered stable when the spatial positions of all atoms are fixed, and the system as a whole reaches the lowest energy state. After convergence testing, geometry optimization is an essential step to ensure the stability of the structure.

In the calculations, the total energy plane-wave pseudopotential method was used, employing ultrasoft pseudopotentials to describe the interaction between ions and valence electrons while neglecting the effects of core electrons. The exchange-correlation energy between electrons was corrected using the generalized gradient approximation (GGA)^[10]. The pseudopotential function was selected from the CASTEP-provided set, and the exchange-correlation functional was chosen as the PBE method within the gradient-corrected functional^[11,12]. In the theoretical calculations, the crystal wavefunctions were expanded using a plane-wave basis set, with a plane-wave cut-off energy of 500.0 eV and a k-point mesh density of 3×3×3. The BFGS method was used to optimize the structure to its lowest energy point, with

the convergence criteria set as follows: Energy: 1.0×10^{-5} eV/atom, Max. force: 0.3 eV/nm, Max. stress: 0.05 GPa, Max. displacement: 0.0001 nm, Max. iterations: 100. The optimized structures are shown in Figure 3. Table 3 summarizes the total energy of these six structures, with the structure having the lowest energy (structure e) being selected for further calculation of its mechanical properties. The calculated values for the bulk modulus (B), shear modulus (G), Young's modulus (E), and Poisson's ratio (ν) are presented in Table 4.

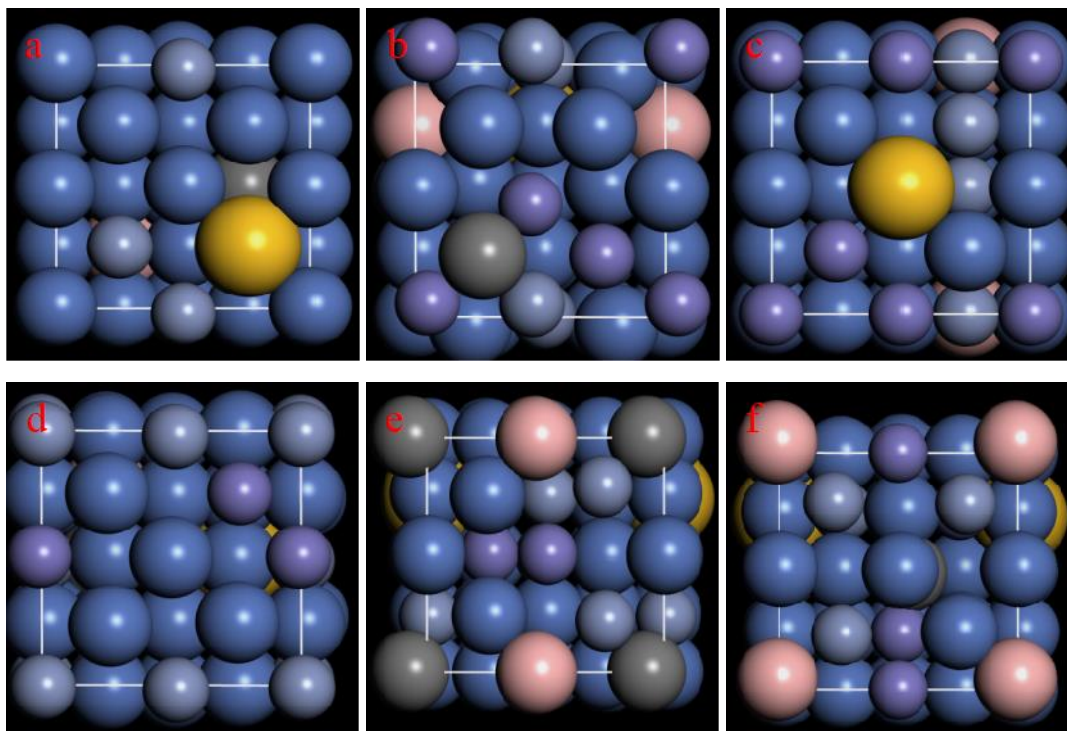


Fig. 3 Optimized Structural Diagram

Table 3 Final State Energy of all structure

Structure	a	b	c	d	e	f
Energy (eV)	-43226.50	-43225.83	-43226.20	-43226.05	-43225.55	-43226.07

Table 4 Mechanical Property Parameters

B/GPa	G/GPa	E/GPa	ν
209.84465	76.48284	204.37692	0.3361

5 OBTAINS MECHANICAL PROPERTIES PARAMETERS BY JMATPRO

JMatPro is a powerful material property simulation software, widely used for phase diagram calculations and alloy property predictions. This software excels in areas such as material composition design, process optimization, and performance prediction, and has been extensively applied in both research and engineering fields^[13].

Based on the element ratios and grain sizes modeled using first-principles calculations, the parameters were input into the JMatPro software. The mechanical property parameters obtained from the first-principles calculations were used to calibrate the JMatPro model. Subsequently, the Strength and Hardness module in JMatPro was utilized to compute the stress-strain curve of the laser cladding layer, as shown in Figure 4.

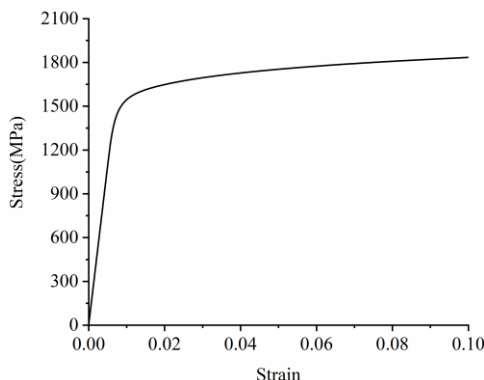


Fig.4 stress-strain curves

Metal cutting processes are typically accompanied by high temperatures and high strain rates. Using the High Temperature Strength module in JMatPro, stress-strain curves under different temperatures and strain rates were calculated, as shown in Figure 5.

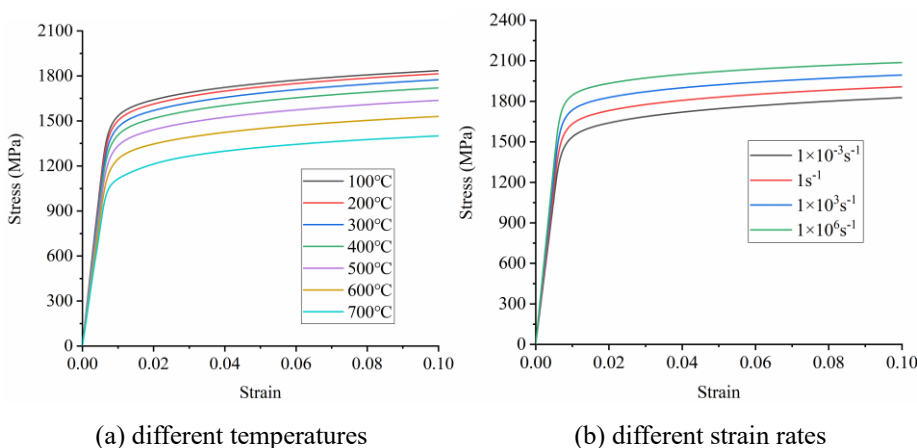


Fig.5 stress-strain curves

6 DETERMINATION OF JOHNSON-COOK CONSTITUTIVE PARAMETERS

The Johnson-Cook constitutive model is simple in form, highly accurate, and its strain rate and temperature range closely align with those encountered in cutting processes. As a result, it is widely used in finite element simulations of machining^[14,15]. Therefore, the Johnson-Cook constitutive model was selected to characterize the mechanical properties of the laser cladding material. Its mathematical expression is given by Equation (1.1), where the five constitutive parameters are A, B, C, m and n . Using JMatPro, stress-strain curves under different conditions can be obtained, and these curves can be used for parameter fitting to calculate the Johnson-Cook constitutive parameters.

$$\sigma = (A + B\varepsilon^n) (1 + C \ln \dot{\varepsilon}^*) (1 - T^{*m}) \tag{0.1}$$

In the equation, σ represents the yield strength of the material, ε is the equivalent plastic strain, $\dot{\varepsilon}^* = \dot{\varepsilon} / \dot{\varepsilon}_0$ is the dimensionless plastic strain rate, where $\dot{\varepsilon}_0$ is the reference strain rate. Additionally, n is the strain hardening exponent, C is the strain rate sensitivity coefficient, and m is the thermal softening exponent. $T^* = (T - T_r) / (T_m - T_r)$, T_r is the reference temperature, T_m is the melting point

temperature of the material, and A, B, C, m, n are the constitutive parameters^[16].

In this case, A represents the yield strength under reference temperature and quasi-static conditions is directly obtained from Figure 4 as $A=1368.7$ MPa. After neglecting the material's strain rate hardening and thermal softening effects^[17], by fitting the stress-strain data from the strengthening stage under quasi-static conditions to the equation, the parameter $B=755.5$ MPa, $n=0.252$. Ignoring the thermal softening effect, the fitted values of A, B , and n were substituted into the equation. Using strain rates of $1 \times 10^{-3} \text{ s}^{-1}$, 1 s^{-1} , $1 \times 10^3 \text{ s}^{-1}$, $1 \times 10^6 \text{ s}^{-1}$, stress data at a strain of 0.1 were fitted to obtain $C=0.0092$. Finally, by fitting the stress data at a strain of 0.1 for temperatures of 100°C, 200°C, 300°C, 400°C, 500°C, 600°C, and 700°C, the thermal softening coefficient m was determined as 1.77.

After determining all the Johnson-Cook constitutive model parameters, these parameters are substituted into the original Johnson-Cook constitutive model, resulting in the constitutive model for the laser cladding layer:

$$\sigma = (1368.7 + 755.5\varepsilon^{0.252}) \left(1 + 0.0092 \ln \dot{\varepsilon}^*\right) \left(1 - T^{*1.77}\right) \quad (0.2)$$

7 CONCLUSION

A crystal model of Ni-based alloys was established using the first-principles calculation software MS, and necessary convergence tests for the cutoff energy and k-point in the Brillouin zone were performed. Elastic constants were then calculated for the optimized structure. The obtained mechanical property parameters were integrated with JMatPro to generate stress-strain curves for the cladding layer under different temperatures and strain rates, and the Johnson-Cook constitutive parameters were fitted to derive the constitutive model for the cladding layer. This approach not only enhances the accuracy of the constitutive parameters but also significantly reduces experimental costs and time consumption. The results demonstrate that this method effectively supports the precise description of material properties in finite element simulations, providing a theoretical foundation for the finite element simulation of machining processes for Ni-based cladding layers.

ACKNOWLEDGMENTS

This study was supported by National Natural Science Foundation of China (Grant nos. 51875409, 52275366), Tianjin Education Commission Project (2020ZD08), Tianjin innovation team project (XC202051), the Tianjin Post graduate Research and Innovation Project (Grant nos. 2021YJSS217, 2022SKY278, and 2022SKYZ295). This work is also supported by National-Local Joint Engineering Laboratory of Intelligent Manufacturing Oriented Automobile Die & Mould.

REFERENCES

- [1] Liu X Y, Qin L J, Guo Z F, Wang Y, and Lu Z W, "Anti-Friction and Wear Resistance of Ni-Based Soft and Hard Composite Coatings," *Tribology*, vol. 44, pp. 1479-1493, November 2024.
- [2] Li Q, Jin M, Zou Z Y, Guo J, and Yang C, Parameter Determination and Application Research of Mixed Hardening Model Based on Cyclic Tension-compression Test, *Journal of Mechanical Engineering*, vol. 56, pp. 63-68, January 2020.
- [3] Zhou Y C, "Mechanical properties of stainless steel products by additive manufacturing," Zhejiang University, 2020.
- [4] Xia Y, Xu K, Zheng G, Zou R, Li B, and Hu P, "Investigation on the elasto-plastic constitutive equation of parts fabricated by fused deposition modeling" *Rapid Prototyping Journal*, *Rapid Prototyping Journal*, vol. 25, pp. 592-601, January 2019.
- [5] XIE Zhong-ya, "Basic Experimental Study on Machinability of Titanium Alloy by Laser Increasing," Shanghai Jiao Tong University, 2017.
- [6] Wang T, Qiao W, Wang S, Li Z, Wang H, and Lei J, "Ti-6Al-4V alloy fabricated by laser direct deposition: dynamic mechanical properties, constitutive model, and numerical simulation," *Surface Review and Letters*, vol. 27, pp. 1950191, 2020.
- [7] Ma L T, Li Y B, Huang Y, Liu C, Zhang Q and Chen Y, "Adsorption and Occurrence of n-heptadecane in Narrow Slit Pores of Illite," *Journal of Xi'an Shiyou University*, vol. 39, pp. 29-38, November 2024.
- [8] Clark S J, Segall M D, Pickard C J, Hasnip P J, Probert M I, Refson K, and Payne M C, "First principles methods using CASTEP," *Zeitschrift für kristallographie-crystalline materials*, vol. 220, pp. 567-570, 2005.
- [9] Geng H Y, Sluiter M H F and Chen N X, "Cluster expansion of electronic excitations: Application to fcc Ni-Al alloys," *The Journal of chemical physics*, vol. 122, pp. 214706, June 2005.
- [10] Sun, Kioussis and Ciftan, "First-principles determination of the effects of boron and sulfur on the ideal cleavage fracture in Ni₃Al," *Physical review. B, Condensed matter*, vol. 54, pp. 3074-3078, August 1996.
- [11] Perdew J P, Burke K, Ernzerhof M, "Generalized Gradient Approximation Made Simple," *Physical Review Letters*, vol. 77, pp. 3865-3868, October 1996.
- [12] Rabe, Karin M, "Atomic and Electronic Structure of Solids," *Physics Today*, vol. 57, pp. 90-90, 2004.
- [13] Dai S, Yu W, Feng C, "Design of new biomedical titanium alloy based on d-electron alloy design theory and JMatPro software," *Transactions of Nonferrous Metals Society of China*, vol. 23, pp. 3027-3032, October 2013.
- [14] Lu S H, "Constitutive modeling and experimental study of the sawtooth chips in high speed cutting," Nanjing University of Aeronautics and Astronautics, 2009.
- [15] Lu S H, He N, "Experimental Investigation of the Dynamic Behavior of Hardened Steel in High Strain Rate and Parameter Fitting of Constitutive Equation," *China Mechanical Engineering*, vol. 19, pp. 2382-2385, October 2008.
- [16] Johnson G, Cook W, "A constitutive model and data for metals subjected to large strains, high strain rates and high temperatures," *Proceedings of the Seventh International Symposium on Ballistics the Hague*, 1983.
- [17] Liu E L, Xing H W, Wang M M, Xu Z Z and Zhao N, "J-C constitutive modeling of high temperature alloys Inconel625," *The Chinese Journal of Nonferrous Metals*, vol. 28, pp. 732-741, April 2018.